



Design, synthesis and pharmacological screening of novel renoprotective methionine-based peptidomimetics: Amelioration of cisplatin-induced nephrotoxicity

Khalid A. Agha^{a,b,*}, Tarek S. Ibrahim^{b,c}, Nehal M. Elsherbiny^{d,e}, Mohamed El-Sherbiny^{f,g}, Eatedal H. Abdel-Aal^b, Zakaria K. Abdel-Samii^b, Nader E. Abo-Dya^{b,d}

^a Department of Pharmaceutical Organic Chemistry, Faculty of Pharmacy, Fayoum University, Fayoum 63514, Egypt

^b Department of Pharmaceutical Organic Chemistry, Faculty of Pharmacy, Zagazig University, Zagazig 44519, Egypt

^c Department of Pharmaceutical Chemistry, Faculty of Pharmacy, King Abdulaziz University, Jeddah 21589, Saudi Arabia

^d Department of Pharmaceutical Chemistry, Faculty of Pharmacy, Tabuk University, Tabuk 71491, Saudi Arabia

^e Department of Biochemistry, Faculty of Pharmacy, Mansoura University, Mansoura 35516, Egypt

^f Department of Anatomy, Faculty of Medicine, Mansoura University, Mansoura 35516, Egypt

^g College of Medicine, AlMaarefa University, Riyadh 11597, Saudi Arabia

ARTICLE INFO

Keywords:

Nephrotoxicity
Methionine
Peptidomimetics
Benzotriazole
Antioxidative stress potential
Cisplatin

ABSTRACT

Cisplatin (CP) is an effective chemotherapeutic agent for treatment of various types of cancer, however efforts are needed to reduce its toxic side effect. Previous studies revealed promising effect of peptides in decreasing CP induced nephrotoxicity. Herein, novel Met-based peptidomimetics were synthesized using *N*-acylbenzotriazole as acylating agent in high yield. Evaluation of renoprotective effect of the synthesized targets on CP treated kidney cell line (LLC-PK1) revealed that pretreatment with 1/3 IC₅₀ of targets **II**, **IIIa-g** attenuated CP induced cell death where the IC₅₀ of CP was raised from 3.28 μM to 9.25–41.1 μM. The most potent compounds **IIIg**, **II** and **IIIb** exhibited antioxidative stress in CP-treated LLC-PK1 cells as confirmed by raising GSH/GSSG ratio and SOD concentration as well as decreasing ROS and MDA. Additionally, *in vivo* experiments using Sprague Dawley rats showed renoprotective effect of **IIIg** against CP-induced nephrotoxicity as evidenced by improved results of renal function tests and attenuated CP-induced renal structural injury. Moreover, antioxidant activity of **IIIg** was demonstrated via its ability to reduce renal MDA level and up-regulate renal antioxidant element GSH level. Further, immunohistochemistry of renal specimens showed the ability of **IIIg** to restore CP-induced suppression of Nrf2. Interestingly, *in vivo* and *in vitro* studies demonstrated that **IIIg** had no effect on CP antiproliferative activity. An assessment of the ADMET properties revealed that targets **IIIg**, **II** and **IIIb** showed good drug-likeness in terms of their physicochemical, pharmacokinetic properties. The findings presented here showcase that **IIIg** is a promising renoprotective candidate with antioxidative stress potential.

1. Introduction

Cis-diamminedichloroplatinum (Cisplatin; CP) is an effective chemotherapeutic agent; it is effectively used in the treatment of bladder, cervix, lung and head cancer [1]. However, the clinical importance of CP is limited by dose dependent adverse effects. Kidney toxicity is the main side effect, which may lead to renal failure and even death on exposure to high dose or prolonged use of CP [2,3].

The uptake of CP by renal tubular epithelial cells involves special membrane transporters where it undergoes activation into more toxic

products. This induces nephrotoxicity by multitude of mechanisms including DNA damage, mitochondrial apoptosis pathway and inflammation [4,5]. Oxidative stress has been also implicated in CP-induced nephrotoxicity and lead to other associated damage mechanisms such as inflammation and mitochondrial dysfunction [4,6]. Production of reactive oxygen species (ROS) in the cell is balanced with antioxidant defense system, however overproduction of ROS results in cellular damage [7]. Therefore, anti-oxidant and anti-inflammatory agents presented a promising chemopreventive approach against CP-induced nephrotoxicity [8].

* Corresponding author at: Department of Pharmaceutical Organic Chemistry, Faculty of Pharmacy, Fayoum University, Fayoum 63514, Egypt.

E-mail address: Aghanet2010@yahoo.com (K.A. Agha).

<https://doi.org/10.1016/j.bioorg.2021.105100>

Received 20 April 2021; Received in revised form 13 June 2021; Accepted 14 June 2021

Available online 17 June 2021

0045-2068/© 2021 Elsevier Inc. All rights reserved.

During the last three decades considerable interest has been focused on development of new therapeutics based on native and modified peptides. Among these effort Stefanucci group investigated the anti-nociceptive and antioxidant activities of some peptides derived from the enzymatic digestion of soy proteins namely rubiscolin-6, soymorphin-6 and their C-terminal amides.[9] Also attempt to develop endomorphin analogues was studied based on peptidomimetic approach.[10]

It was shown that amino acids (AAs) like methionine, cysteine, arginine, glycine, glutamine and amino acid derivatives like *N*-benzoyl or *N*-acetyl derivatives have the ability to attenuate CP induced nephrotoxicity (Fig. 1) [11,12]. A part of this effect may arise from acting as scavenger of oxygen free radicals or it is related to enhancing GSH production. The oxidation of surface-exposed methionine (Met) residues of proteins by reactive oxygen species (ROS) generates mixtures of the R- and S-isomers of methionine sulfoxide (MetO) [13]. Loss of biological activity of the oxidized protein occurs, due to changes in hydrophobicity and protein conformation [14,15]. However, unlike the ROS-dependent oxidation of other AAs residues of proteins (except cysteine residues), the oxidation of Met residues is readily reversed by the action of methionine sulfoxide reductase (Msr) that catalyzes reduction of MetO residues of proteins back to Met, thereby ROS loses its activity [16,17]. Synergistic antioxidant activity was observed upon screening of dipeptides containing methionine like Met-Met and Met-Trp. Also, administration of CP in the form of CP-Met substitution complex, can reduce CP-induced nephrotoxicity without diminishing the antitumor activity [18,19]. Met significantly improved polymyxin-induced nephrotoxicity and reduced mitochondrial superoxide production in renal tubular cells [20]. Moreover, several studies had confirmed the anti-inflammatory activities of Met and their derivatives in animal models [21–23].

The present study was conducted to alleviate the nephrotoxicity of CP by incorporating a renoprotective and antioxidant AA Met in a dipeptide of additional antioxidant amino acids. *p*-Chlorobenzoyl group was included to improve pharmacokinetics properties of peptides (Fig. 2).

N-acylbenzotriazoles were used as acylating agents to prepare the targets. *N*-acylbenzotriazoles showed numerous merits in peptide or peptidomimetic synthesis such as: (i) chirality is preserved during the course of their preparation and reaction (ii) they form crystals easily; (iii) they are stable in air; and (iv) they are usually isolated in high yields [24].

2. Results and discussion

2.1. Chemistry

N-*p*-Chlorobenzoyl-L-methionine **II** was prepared by the reaction of

N-*p*-chlorobenzoylbenzotriazole **Ia** that was prepared by reported Katritzky benzotriazole methodology [25] with L-methionine in the presence of TEA. AAs like arginine, glycine, cysteine, histidine, phenylalanine and anthranilic acid that have antioxidant or metal chelating activities were coupled to *N*-*p*-chloro-L-methionine **II**. To do this, *N*-*p*-chlorobenzoyl-L-methionine was activated for coupling reaction by its reaction with four equivalent of 1*H*- benzotriazole and one equivalent thionylchloride in CH₂Cl₂ at 25 °C for 3 h to give the corresponding *N*-acylbenzotriazole **IIa** in 85% yield (Scheme 1, Fig. 3).

2.2. Pharmacokinetic and physicochemical screening

Upon administration of a drug, its pharmacokinetics and physicochemical properties influence its rate of absorption, distribution, metabolism and excretion in human system [26–28]. The Lipinski's rule of five is generally used to predict the drug-likeness of a chemical compound by measuring the biological activity, good oral bioavailability together with the compounds tendency to cross various aqueous and lipophilic barriers by adhering to certain conditions [29]. SwissADME was used to predict the pharmacokinetic and physicochemical properties of the compounds [30]. As shown in Table 1, all the compounds obey Lipinski rule of five. Compounds **II**, **IIIa**, **IIIe** and **IIIg** showed high gastro-intestinal absorption. These favourable properties suggest that these compounds could be potential drugs. On the other hand absence of *p*-chlorobenzoyl moiety resulted in low value of LogP_{o/w} indicating highly hydrophilic compounds that will cleared rapidly from the body resulting in poor pharmacokinetic properties.

2.3. Cell-based renoprotective screening

2.3.1. Cell based assay of renoprotection against CP-induced nephrotoxicity using kidney epithelial cells (LLC-PK1)

To verify the renoprotective effect of the synthesized compounds, cell based kidney protection screening was performed using kidney epithelial cells (LLC-PK1). Cell Line cells were obtained from American Type Culture Collection, cells were cultured using Dulbecco's Modified Eagle's Medium (DMEM) (Invitrogen/Life Technologies) supplemented with 10% fetal bovine serum (FBS) (Hyclone), 10 µg/ml of insulin (Sigma), 1% penicillin and streptomycin. All of the other chemicals and reagents were from Sigma, or Invitrogen. The LLC-PK1 cells were treated with various concentrations (100, 25, 6.25, 1.56, 0.39 µM) of synthesized compounds or CP then subjected to 3-(4,5-dimethylthiazol-2-yl)-2,5-diphenyltetrazolium bromide (MTT) assay to determine their IC₅₀ (Table 2). Subsequently LLC-PK1 cells were co-treated with safe doses 1/3 IC₅₀ of the synthesized compounds and different concentration of CP (100, 25, 6.25, 1.56, 0.39 µM) then cell viability and IC₅₀ of CP were measured (Table 2, Fig. 4).

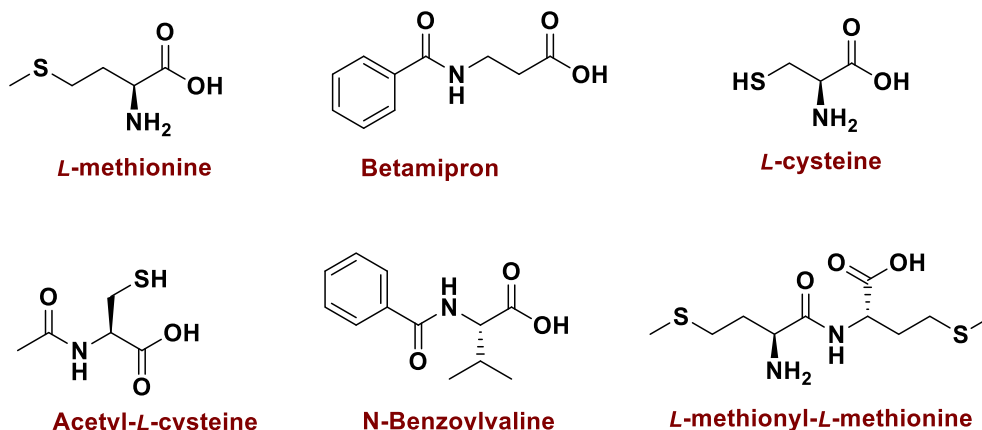


Fig. 1. Example of renoprotective compounds.

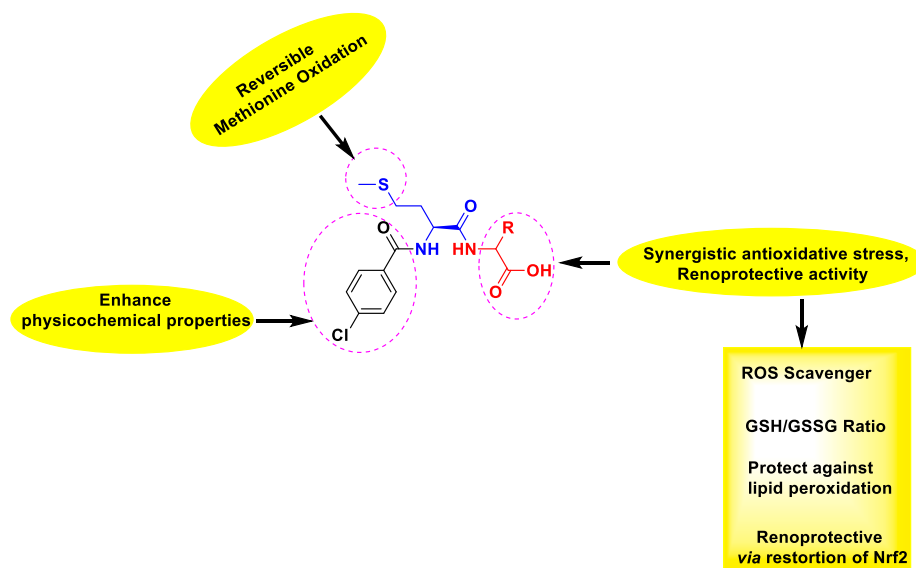
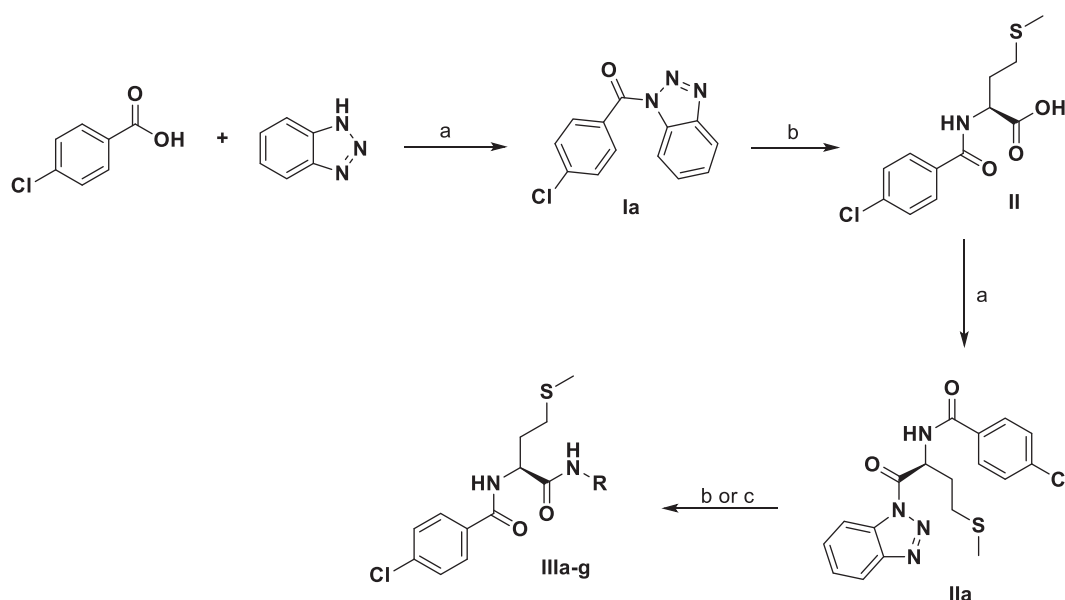


Fig. 2. Proposed mechanisms for renoprotective efficacy of peptidomimetics.



Scheme 1. Chemical synthesis of target compounds, Reagent condition: a) SOCl_2 (1 eq) in CH_2Cl_2 , rt, 3 h, b) L-methionine, TEA (1:1), in $\text{CH}_3\text{CN} / \text{H}_2\text{O}$ (3:1), rt, 5 h. c) various amino acids in Dioxane / H_2O (3:1), TEA (1 eq), 60°C , 5 h.

The IC_{50} of CP group was $3.28 \pm 0.09 \mu\text{M}$. Upon mixing CP with 1/3 IC_{50} of the target peptidomimetics cell viability was enhanced and the IC_{50} (Fig. 4) was increased from three fold ($\text{IC}_{50} = 9.2 \mu\text{M}$, CP + compound IIIa) to about 13 fold ($\text{IC}_{50} = 41.1 \mu\text{M}$, CP + compound IIIg). Such enhancement in cell viability by rise in CP IC_{50} confirms that the Met-containing peptidomimetics protect LLC-PK1 cells against the cytotoxic effects of CP. Compound IIIg provides the best renoprotective effect amongst the tested compounds and its calculated physicochemical and pharmacokinetic properties were optimum for a drug candidate.

2.3.2. Effect of the synthesized peptidomimetics on oxidative stress in CP-treated LLC-PK1 cell

In an attempt to gain insight about the mechanism by which the targets exert renoprotective effect, LLC-PK1 cell line was treated with 1/3 IC_{50} of the most potent targets II, IIIb and IIIg respectively for 8 hr, followed by addition of $4 \mu\text{M}$ of CP and the mixture was left for 24 hr. Oxidative stress biomarkers namely, GSH/GSSG ratio, ROS, SOD and

MDA were measured at the beginning of the experiment, after 8 h and at the end of the experiment (Table 3, Fig. 5). Effect of synthesized peptidomimetics on oxidative stress is unblemished as following:

2.3.2.1. GSH/glutathione disulfide (GSSG) ratio. Glutathione is a tripeptide observed in all cells except erythrocytes and it plays a vital role in various processes as free radical scavenger, inhibitor of lipid peroxidation and in detoxification [31]. The ratio of reduced GSH to oxidized GSH (GSSG) is an indicator of cellular health; this ratio is reduced in neurodegenerative diseases and in tissue or cells under oxidative stress such as our model [32,33]. Treatment of LLC-PK1 cells with CP for 8 hrs, significantly lowered the initial GSH/ GSSG (3.73 ± 0.153) to 0.53 ± 0.12 . Upon increasing the time of exposure of LLC-PK1 to CP for additional 24 hrs the ratio of GSH/ GSSG was further decreased to 0.37 ± 0.06 . When cells were treated with compounds IIIg, II and IIIb for 8 hrs, followed by subsequent treatment with CP for 24 hrs, targets IIIg, II and IIIb maintained the level of GSH/ GSSG to fivefold, fourfold

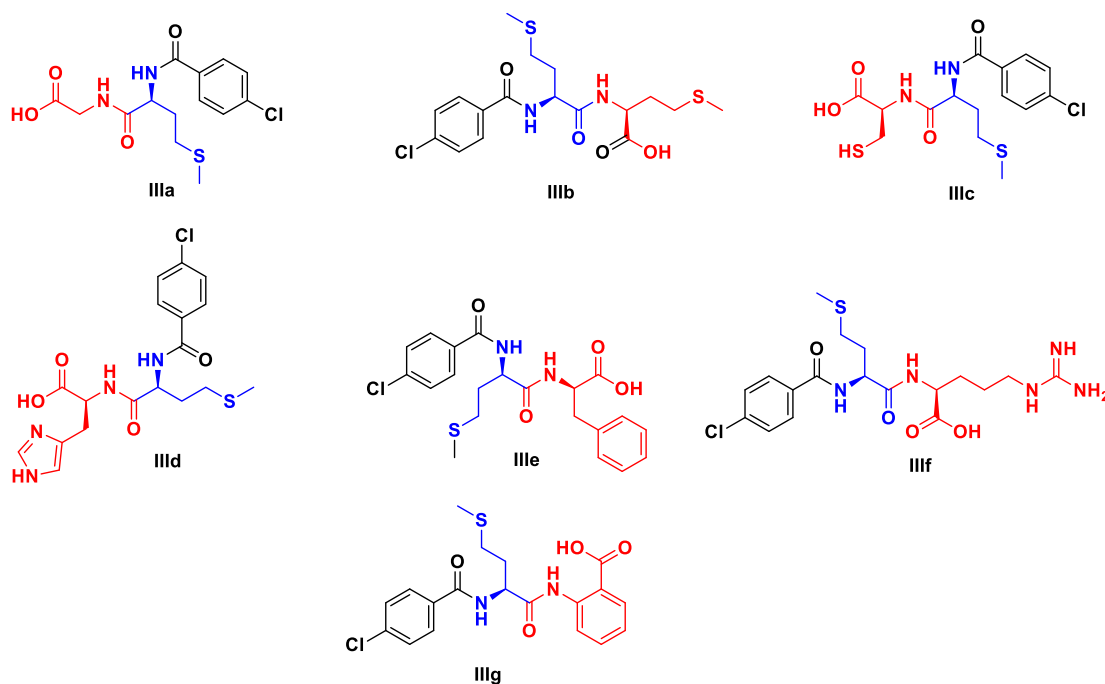


Fig. 3. Chemical structure of the designed methionine based peptidomimetics.

Table 1
Predicted physicochemical properties of synthesized peptidomimetics.

Physicochemical properties	Compounds							
	II	IIIa	IIIb	IIIc	IIId	IIIe	IIIf	IIIg
Molecular weight (g/mol)	287.76	344.81	418.96	390.91	424.90	434.94	443.95	406.88
Num. heavy atoms	18	22	26	24	28	29	29	27
Num. arom. heavy atoms	6	6	6	6	11	12	6	12
Num. rotatable bonds	7	10	13	11	12	12	15	10
Num. H-bond acceptors	3	4	4	4	5	4	5	4
Num. H-bond donors	2	3	3	3	4	3	6	3
Molar Refractivity	73.04	85.65	107.67	98.39	107.09	114.95	113.98	107.25
TPSA (\AA^2)	91.70	120.80	146.10	159.60	149.48	120.80	182.70	120.80
Consensus $\text{Log}P_{o/w}$	2.24	1.76	2.56	1.96	1.72	3.12	1.38	3.18
Consensus $\text{Log}P_{o/w}$ if <i>p</i> -chlorobenzoyl group removed from the desined peptidomimetic	-0.59	-0.84	0.08	-0.69	-0.78	0.71	-1.06	1.03
GI absorption	High	High	Low	Low	Low	High	Low	High
BBB permeant	No	No	No	No	No	No	No	No
Lipinski	Yes	Yes	Yes	Yes	Yes	Yes	Yes	Yes

Table 2
Renoprotective effect of synthesized peptidomimetic on CP treated LLC-PK1 cells.

Compound	IC ₅₀ before mix (μM)	Safe conc. (μM)	Cisplatin IC ₅₀ after mix
II	93 \pm 2.66	30	18.7 \pm 0.54
IIIa	55.8 \pm 1.59	15	9.27 \pm 0.27
IIIb	90.6 \pm 2.59	30	16.9 \pm 0.48
IIIc	38.7 \pm 1.11	12	11.0 \pm 0.31
IIId	21.5 \pm 0.61	7	12.8 \pm 0.37
IIIe	28.8 \pm 0.82	10	12.6 \pm 0.36
IIIf	76 \pm 2.17	25	14.7 \pm 0.42
IIIg	157 \pm 4.5	50	41.1 \pm 1.18
Cisplatin	3.28 \pm 0.09	-	-

and three fold that of CP group respectively (Fig. 5). Compound IIIg is the most potent in inhibition of glutathione depletion and this may contribute to explanation of its potent renoprotective effect against CP toxicity.

2.3.2.2. *Superoxide dismutase (SOD)*. SOD plays a key role in guarding against oxygen radicals. It was proved that, increasing the level of free

radicals decreases the level of SOD also CP treatment negatively affect SOD level negatively [34,35]. Data in table 3 showed that CP lowered SOD level in LLC-PK1 cells, this effect was reversed by pretreatment with compounds IIIg, II and IIIb. Compounds IIIg and II were highly active in raising the level of SOD to more than four and threefold (21.43 ± 0.15 , 24.87 ± 0.06) respectively with respect to CP only treated cells (6.27 ± 0.15) (Fig. 5).

2.3.2.3. *Malondialdehyde (MDA)*. Free radicals initiate lipid peroxidation that can affect ion exchange in the cell membrane and can lead to adverse effects[36]. This process can be monitored by measuring the level of their end product (MDA) [37]. CP increased the level of MDA [38] to fourfold after 8 hr and up to six fold at the end of experiment. Pretreatment with the synthesized peptidomimetics II, IIIb and IIIg 8 hrs prior to addition of CP reduced the level of produced MDA to 20.43 ± 0.15 , 25.6 ± 0.2 and 18.67 ± 0.21 respectively (about half the MDA level in CP group 38.5 ± 2.92) (Fig. 5).

2.3.2.4. *Reactive oxygen species (ROS)*. Oxidative stress is characterized by elevated intracellular levels of reactive oxygen species (ROS) that produce damaging effect to lipids, proteins and DNA [39,40]. CP in the

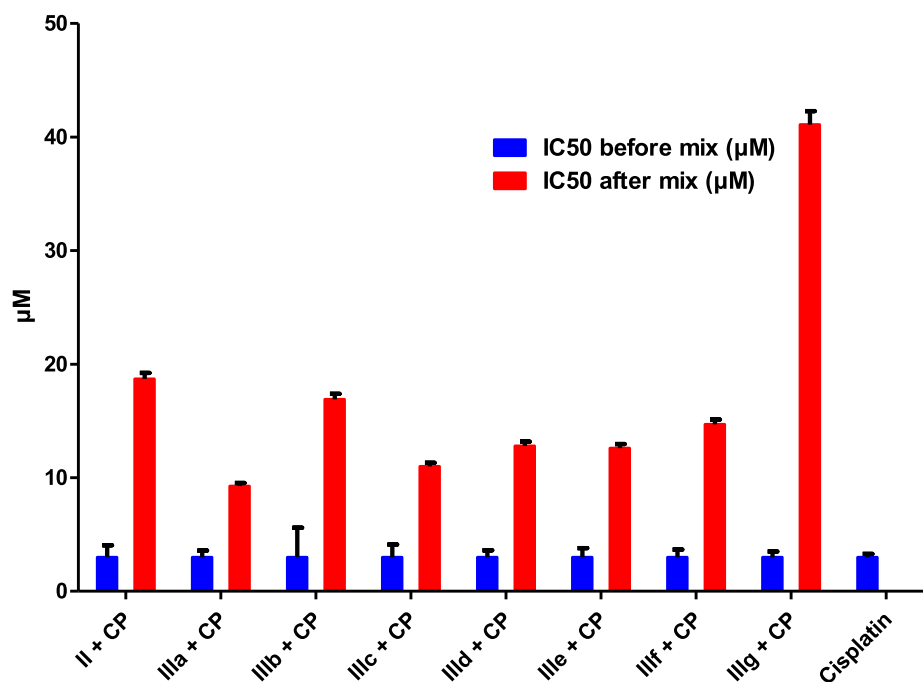


Fig. 4. The protective effect of peptidomimetic on CP-induced nephrotoxicity.

Table 3

Effect of synthesized peptidomimetics **II**, **IIIb**, **IIIg** on oxidative stress biomarkers GSH/GSSG ratio, SOD, MDA, ROS.

Oxidative stress biomarkers*	Group								
	Control	Cisplatin (8 hr)	II (8 hr)	IIIb (8 hr)	IIIg (8 hr)	CP (24 hr)	CP + II (24 hr)	CP + IIIb (24 hr)	CP + IIIg (24 hr)
GSH/GSSG RATIO*	3.73 ± 0.153	0.53 ± 0.12	2.9 ± 0.1	1.93 ± 0.06	3.33 ± 0.12	0.37 ± 0.06	1.67 ± 0.12	1.13 ± 0.06	1.97 ± 0.06
SOD (U / ml)*	41.37 ± 0.31	11.43 ± 0.15	27.33 ± 0.15	19.97 ± 0.15	29.87 ± 0.21	6.27 ± 0.15	21.43 ± 0.15	14.67 ± 0.12	24.87 ± 0.06
MDA (ng /ml)*	6.9 ± 0.2	26.83 ± 0.15	15.27 ± 0.15	18.43 ± 0.15	12.17 ± 0.15	38.5 ± 2.92	20.43 ± 0.15	25.6 ± 0.2	18.67 ± 0.21
ROS (U/L)*	8.93 ± 0.153	34.43 ± 0.21	17.77 ± 0.15	22.97 ± 0.12	15.37 ± 0.06	45.8 ± 0.2	26.17 ± 0.12	29.97 ± 0.21	24.67 ± 0.12

*GSH/GSSG glutathione/glutathione disulfide ratio, SOD Superoxide dismutase, MDA Malondialdehyde, ROS reactive oxygen species

current study generated ROS more than fivefold the untreated LLC-PK1 cells. Prior treatment of LLC-PK1 cells with peptidomimetics **II**, **IIIb** and **IIIg** before CP addition reduced ROS production to about half with compounds **IIIg**, **II** and **IIIb** (24.67 ± 0.12 , 26.17 ± 0.12 and 29.97 ± 0.21) respectively (Fig. 5). The results obtained during this stage of experiment prove the presence of antioxidative stress properties of the synthesized peptidomimetics that help as a guard against oxidative stress produced by CP.

2.4. In vivo screening

2.4.1. Assessment of potential toxicity of IIIg

2.4.1.1. Experimental design. All experimental procedures were aligned with the guidelines of the ethics committee at Faculty of Medicine, Mansoura University, Egypt. Sprague-Dawley rats were maintained at standard conditions of humidity and temperature with free access to food and water. After one week of acclimatization, a toxicity study to assess the possible *in vivo* toxic effect of **IIIg** was performed. For this purpose, 24 animals were randomly assigned into three groups receiving different concentration of **IIIg** as following:

Group I: received **IIIg** at a dose (0.068 gm/kg/day) for 10 days

Group II: received **IIIg** at a dose (0.136 gm/kg/day) for 10 days

Group III: received **IIIg** at a dose (0.273 gm/kg/day) for 10 days

Additional untreated group that received vehicle only for 10 days was used as normal control.

At the end of the experimental protocol, animals were sacrificed using high dose thiopental (40 mg/kg), blood samples were withdrawn and centrifuged for 10 min at 3000 rpm to separate serum for further analysis of liver and kidney functions. Liver and kidney specimens were excised and fixed in 10% buffered formalin for histological analysis.

2.4.2. Assessment of biochemical markers of kidney function

Serum levels of creatinine (Cr) and blood urea nitrogen (BUN) (Bio-med, Egypt) were assessed based on manufacturers' instructions.

2.4.3. Assessment of biochemical markers of liver function

Serum levels of alanine aminotransferase (ALT) and aspartate aminotransferase (AST) (Biodiagnostics, Giza, Egypt) were evaluated by colorimetric method according to manufacturers' instructions.

2.4.4. Histopathological studies

Fixed liver and kidney specimens were embedded in paraffin sections and cut into 5- μ m thick sections. Sections were then stained with hematoxylin and eosin (H&E) and viewed under light microscope. Images were captured using a digital camera-aided computer system (Nikon digital camera, Tokyo, Japan).

2.4.5. Results

As shown in Table 4 and Fig. 6, the highest dose of **IIIg** produced moderate liver and kidney toxicity, where rats in group III showed significant increase in liver and kidney function indices when compared to

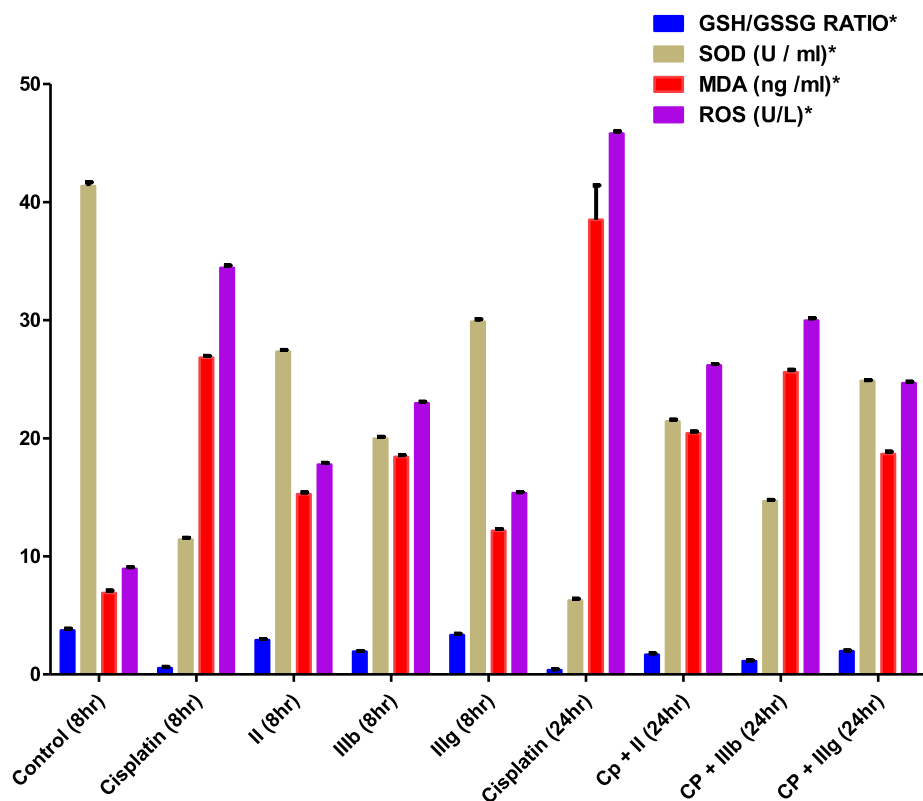


Fig. 5. Effect of synthesized Met-based peptidomimetic II, IIIb and IIIg on oxidative stress biomarkers (GSH/ GSSG ratio, SOD, MDA and ROS) in CP-treated LLC-PK1 cells.

Table 4

Effect of different doses of IIIg on liver and kidney function tests.

	GPT (U/L)	GOT (U/L)	Cr (mg/dl)	BUN (mg/dl)
Control	23.66 ± 5.8	89.67 ± 4.05	0.52 ± 0.03	16.47 ± 1.4
Group I	24 ± 5.2	99.33 ± 9.3	0.57 ± 0.04	16.67 ± 3.9
Group II	28 ± 5.5	105.3 ± 9.3	0.61 ± 0.06	19.33 ± 4.9
Group III	45.3 ± 1.7*	126.7 ± 8.09*	0.92 ± 0.1*	34.67 ± 0.3*

*Significant compared to control group at $p \leq 0.05$

control group ($p < 0.05$). Additionally, histopathological study demonstrated glomerular, tubular and hepatic changes. Of note, one rat died from group III during the experimental course.

Based on the aforementioned results, the middle dose (0.136 gm/kg/day) was used to assess the potential *in vivo* renoprotective effect of the synthesized peptidomimetic IIIg in CP-induced renal toxicity according to the following protocol:

2.5. Assessment of potential renoprotective efficacy of IIIg using CP-induced renal toxicity model

2.5.1. Experimental design

All experimental procedures adhered to the guidelines of the ethics committee at Faculty of Medicine, Mansoura University, Egypt. Twenty four male Sprague-Dawley rats were randomly assigned after acclimatization for one week into the following groups.

Normal control group: received vehicle only for 10 constitutive days.

Cisplatin group: Rats received CP (10 mg/kg, once, ip) on day 6.

Cisplatin + Methionine: received Met (100 mg/kg/day, ip) for 10 days and cisplatin on day 6 of drug administration.

Cisplatin + IIIg: Rats received IIIg (0.136 gm/kg/day, ip) for 10 constitutive days and CP on day 6 of IIIg administration.

At the end of the experimental protocol, animals were sacrificed using high dose thiopental (40 mg/kg), blood samples were withdrawn and centrifuged for 10 min at 3000 rpm to separate serum for further analysis of kidney functions. kidneys were excised. One part was homogenized in phosphate buffered saline for further analysis of MDA and GSH, and the other part was fixed in 10% buffered formalin for histological analysis and immunohistochemical studies.

2.5.2. Assessment of oxidative stress in renal tissue

Level of MDA and GSH in renal tissue homogenate was assessed

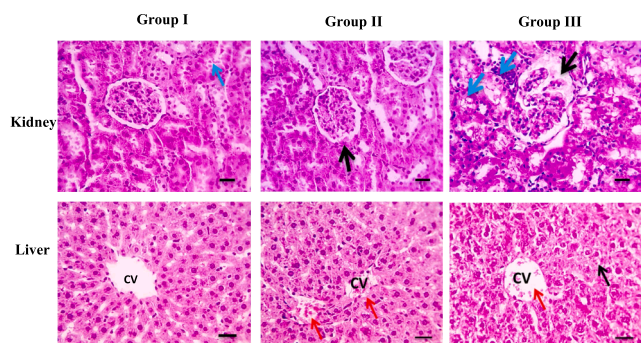


Fig. 6. Upper panel: Microscopic pictures of H&E stained kidney sections showing normal glomeruli and tubules in group I, normal tubules and minute dilation of Bowman's capsule in group II and dilation of Bowman's capsule with eosinophilic material (black arrow) accompanied with mild tubular degeneration (blue arrows) in group III. Lower panel: Microscopic pictures of H&E stained liver sections showing normal radiating hepatic cords around central veins (CV) in group I, normal hepatocytes and mildly congested CV (red arrows) in group II and mildly congested CV (red arrows) and mild hepatocytes degeneration in group III. X:400 bar 500. (For interpretation of the references to colour in this figure legend, the reader is referred to the web version of this article.)

using commercially available colorimetric kits purchased from Biodiagnostics (Giza, Egypt) following manufacturers' protocol.

2.5.3. Immunohistochemical study

Five μm renal sections were deparaffinized and blocked with 5% bovine serum albumin for 2 hrs. Thereafter, sections were washed and incubated with primary antibody for Nrf-2 (Abcam, USA, ab89443) overnight at 4 °C. Following incubation, slides were washed and then incubated with labeled secondary antibody for 1 hr and the immunoreaction was visualized using 3,3'-diaminobenzidine (DAB, 2%) as chromogen. Slides were then counterstained by Mayer's hematoxylin and sections were inspected and images were captured using Olympus® digital camera installed on Olympus® microscope.

Assessment of combined **IIIg** administration on CP antiproliferative effect.

Next, we investigated if **IIIg** co-administration affected CP chemotherapeutic efficacy using *in vivo* and *in vitro* Ehrlich Ascites Carcinoma (EAC).

2.5.4. In vivo EAC model

Twenty four adult Swiss albino mice (20–30 gm) were used in this study. The animals were housed under standard conditions of humidity and temperature and allowed free access to regular rodent diet and water. Animals were injected intraperitoneally with suspension EAC cells (2×10^6 viable cells/mouse) under aseptic conditions. Ehrlich-tumor cells were provided by National Cancer Institute (Cairo, Egypt) and maintained by serial intra peritoneal passage in female Swiss albino mice at 7–10 day intervals [41]. Following tumor cells transplantation, the EAC mice were further subdivided into three groups as following:

Untreated EAC mice: received vehicle, ip, daily for 14 days from the 1st day of the experiment.

Cisplatin treated EAC mice: received CP (5 mg/kg, ip, single treatment on the 1st day of the experiment), 1 h prior to the injection of vehicle, ip, daily for 14 days from the 1st day of the experiment.

Cisplatin + **IIIg treated EAC mice:** received CP (5 mg/kg, ip, single treatment on the 1st day of the experiment), 1 h prior to the injection 0.136 gm/kg **IIIg**, ip, daily for 14 days from the 1st day of the experiment.

2.5.5. Assessment of tumor volume

At the end of the experimental procedure, animals were sacrificed under anaesthesia and the ascites fluid was separated individually from each animal by needle aspiration from the peritoneal cavity under aseptic conditions and collected in graduated tubes for tumor volume measurement.

2.5.6. In vitro EAC cells and trypan blue exclusion assay

EAC cells were cultured in 96-well plate (1×10^4 cells/well) and kept at 37 °C for 24 h in 5% CO₂ incubator. Cells were then shifted to serum free medium and treated with CP (10, 50 ad 100 $\mu\text{g}/\text{ml}$) alone and in combination with different concentration of **IIIg** (10, 50 and 100 μM). Five wells were used for each treatment concentration in addition to five wells treated with vehicle only (DMSO, 0.1%). The plate was incubated for 48 h in 5% CO₂ incubator. Effect of treatment on cell viability was determined using trypan blue exclusion assay. Briefly, after appropriate incubation with treatments, equal volumes of trypan blue was added to each well and then Neubauer hemocytometer was used to count number of the stained cells (dead cells) and unstained cells (alive cells). The % of dead EAC cells was then calculated.

2.5.7. Statistical analysis

Results for *in vivo* and *in vitro* experiments were represented as mean \pm SE. Statistical difference among different groups was analyzed by one-way ANOVA test followed by Tukey's post hoc test once differences exist among different experimental groups. GraphPad prism program was used for performing statistical analyses and graphical presentation.

Statistical significance was considered at $p \leq 0.05$.

2.5.8. Results and discussion

As demonstrated in Table 5, cisplatin administration produced marked renal injury as shown by significant increase in serum levels of creatinine and BUN compared to normal group ($p < 0.05$). On the other hand, treatment with Met and Synthesized peptidomimetic **IIIg** improved renal function compared to CP-treated group. However, better results were observed in **IIIg**-treated group. Oxidative stress is a hallmark of CP-induced organ toxicity. Increased lipid peroxidation along with compromised antioxidant defence mechanisms is well established [42]. Similarly, our current study showed marked increase in renal MDA level and significant decrease in renal GSH ($p < 0.05$) compared to normal group. In contrast, treated groups showed significant suppression of MDA level and restoration of GSH level in renal tissue when compared with CP-treated group. Of note, the antioxidant effect observed in synthesized peptidomimetics **IIIg**-treated group was superior compared to methionine group ($p < 0.05$).

The effect of Met and **IIIg** on renal morphological changes induced by CP was shown in Fig. 7. While Fig. 8 showed results of Nrf2 immunostaining in different experimental groups. Nrf2 is a transcription factor that plays a crucial role in regulating redox homeostasis and cellular oxidative defence [43]. A substantial body of literature has reported the role of Nrf2 in safeguarding against CP-induced nephrotoxicity. Indeed, CP renal injury was exacerbated in Nrf2 Knocked out mice [44]. On the other hand, Nrf2 activators demonstrated renoprotective capability against CP-induced toxicity [45]. In this context, Met has been reported to induce Nrf2 and enhance antioxidant defence in rats [46]. Similarly, our results showed decreased immunostaining of Nrf2 in renal tissue of cisplatin treated rats. However, treatment with Met showed mild restoration of Nrf2 immunostaining in renal tissue, while **IIIg** produced more increase in Nrf2 immunostaining in renal tissue of treated rats.

To evaluate the effect of **IIIg** on CP anti-tumor activity, EAC cells were used as *in vivo* and *in vitro* models. EAC is originally a murine spontaneous breast cancer. It is undifferentiated hyperdiploid carcinoma characterized by high transplantable capability, 100% malignancy and rapid proliferation [47,48]. An ascites variant was obtained from EAC spontaneous breast cancer. The ascites was commonly used over the last four decades for assessment of anti-tumor efficacy of various chemicals and natural products. Intraperitoneal inoculation of the ascites produces an ascitic fluid rich in tumor cells. As shown in Fig. 9A, CP antiproliferative efficacy was reflected as significant decrease in tumor volume in cisplatin treated EAC mice compared with untreated EAC mice ($p < 0.05$). However, no significant difference in tumor volume was observed between cisplatin treated EAC mice and cisplatin + **IIIg** treated EAC mice, indicating that **IIIg** had no effect on antiproliferative efficacy of CP. Similar results were obtained *in vitro*, where no significant difference was observed in percentage cell viability between EAC cells treated with CP alone or in combination with **IIIg** at various concentrations, Fig. 9B.

Table 5

Effect of methionine and prepared drug on markers of kidney function (creatinine, BUN) and oxidative stress (MDA, GSH).

	Cr (mg/dl)	BUN (mg/dl)	MDA (nmol/g tissue)	GSH (mmol/g tissue)
Normal	0.55 \pm 0.03	16.25 \pm 3.7	6.7 \pm 1.3	2.9 \pm 0.15
Cisplatin	1.5 \pm 0.15*	82.5 \pm 12.39*	33.66 \pm 4.06*	1.2 \pm 0.2*
Methionine	0.9 \pm 0.05*	46.8 \pm 5.9*	25.9 \pm 2.7*	1.7 \pm 0.3*
IIIg	0.8 \pm 0.04	21.8 \pm 1.7#	14.2 \pm 1.8#	2.8 \pm 0.11#

*Significant compared to control group at $p \leq 0.05$. # Significant compared to methionine group at $p \leq 0.05$.

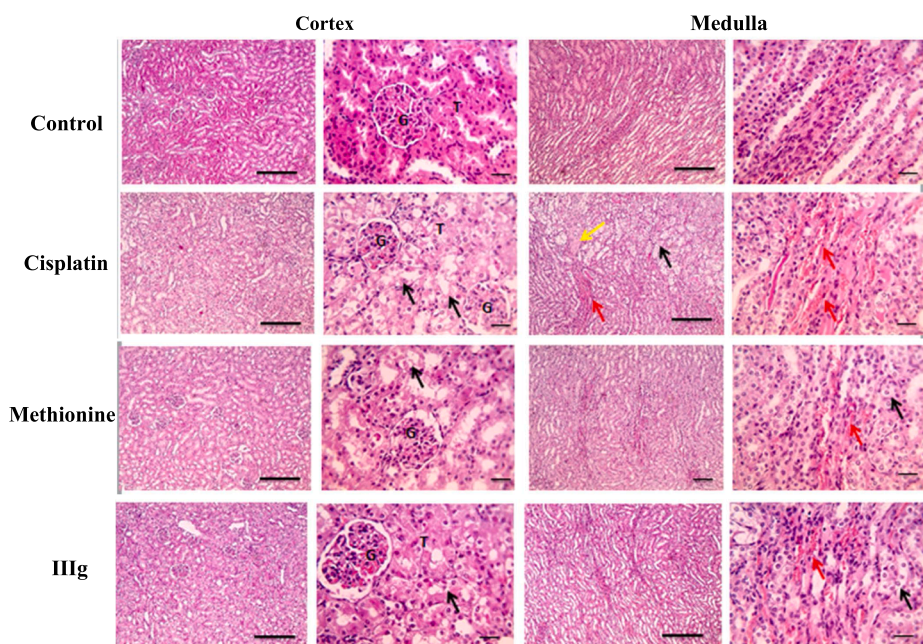


Fig. 7. Microscopic pictures of H&E stained kidney sections showing normal glomeruli (G) and tubules (T) in the control group. Meanwhile, kidney sections from Cisplatin group showed tubular dilation, severe tubular epithelial degeneration (black arrows) in cortex, diffuse tubular epithelial degeneration (black arrows), fibrosis (yellow arrow) with congested blood vessels (red arrows) in medulla. Kidney sections from methionine group showing mild tubular dilation with mild tubular epithelial degeneration (black arrows) in cortex, mild tubular epithelial degeneration (black arrows) and mildly congested blood vessels (red arrows) in medulla. Kidney sections from IIIg group showed mild tubular epithelial degeneration (black arrows) in cortex, mild tubular epithelial degeneration (black arrows) with very mildly congested blood vessels (red arrows) in medulla. Low magnification X: 100 bar 100, high magnification X: 400 bar 50. (For interpretation of the references to colour in this figure legend, the reader is referred to the web version of this article.)

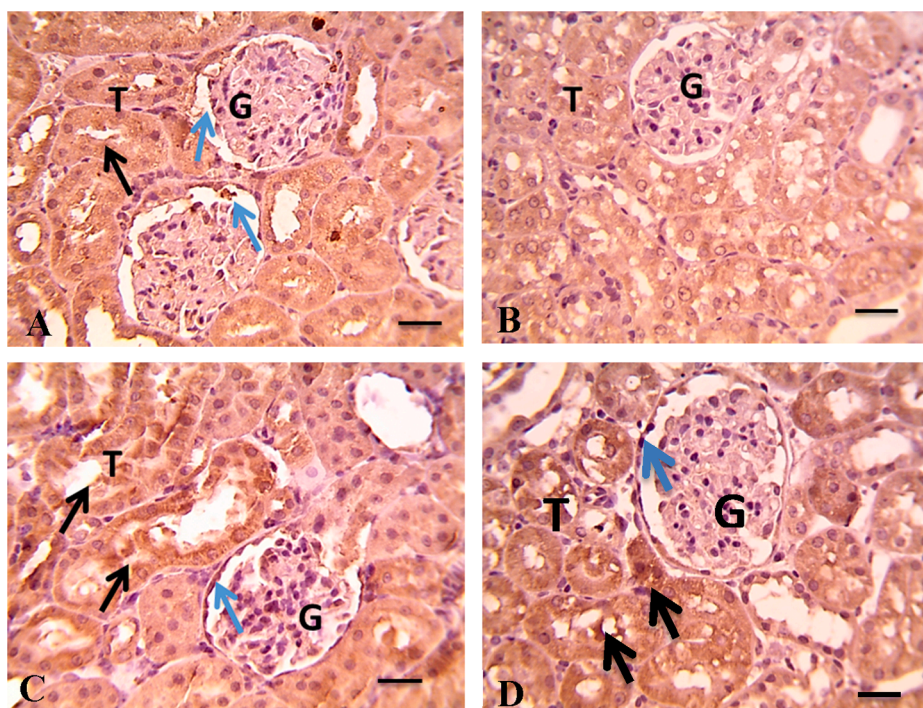


Fig. 8. Microscopic pictures of immunostained renal sections against Nrf2 showing strong positive brown tubular (black arrows) and glomerular (blue arrows) reactions in the normal control group (A). Nrf2 positive tubular and glomerular expression dramatically decreased in Cisplatin group (B). Nrf2 positive tubular (black arrows) and glomerular (blue arrows) expressions mildly increased in Methionine group (C) and moderately increased in IIIg group (D). IHC counterstained with Mayer's hematoxylin. Black arrows point to positive cells. Low magnification X:100 bar 100 and high magnification X:400 bar 50. (For interpretation of the references to colour in this figure legend, the reader is referred to the web version of this article.)

3. Experimental

3.1. General information

Starting materials and solvents were purchased from common commercial sources and used without further purification. Melting points were determined on Fisher melting apparatus and are uncorrected. ^1H NMR (400 MHz) and ^{13}C NMR (100 MHz) spectra were recorded on Bruker a 400 MHz NMR Spectrometer and using $\text{DMSO}-d_6$ as solvent, at Faculty of Pharmacy, Mansoura University. The chemical shift (δ) is reported in ppm, and coupling constants (J) are given in Hz. The HRMS and LC-HRMS were recorded on LC/Q-TOF, 6530 (Agilent Technologies,

Santa Clara, CA, USA) equipped with an autosampler (G7129A), a quat. pump (G7104C) and a column comp (G7116A) at Faculty of pharmacy, Fayoum University. The LC-HRMS analysis was carried out using Zorbax RP-18 column from Agilent Technologies (dimensions: 150 mm \times 3 mm, $dp = 2.7 \mu\text{m}$) and Zorbax Extend-C18 column from Agilent Technologies (dimensions: 50 mm \times 2.1 mm, $dp = 1.8 \mu\text{m}$) in a flow rate of $0.1 \text{ cm}^3/\text{min}$. The mobile phase consisted of a combination of solvent A (water + 0.1% formic acid) and solvent B (acetonitrile + 0.1% formic acid). The elution was as follows: $t = 0 \text{ min}$, 30% B; $t = 1 \text{ min}$, 30% B; $t = 10 \text{ min}$, 70% B. Elemental analysis was performed on the Thermo Fisher Flash 2000 CHNS analyzer at the Regional Center for Mycology and Biotechnology, Al-Azhar University. All reactions were monitored

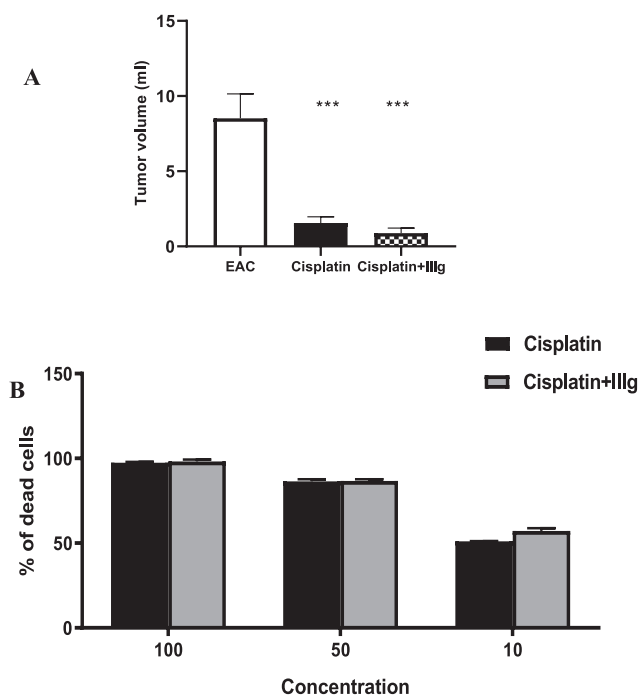


Fig. 9. Effect of co-administration of CP and IIIg on EAC *in vivo* and *in vitro*. A) tumor volume (volume of ascites fluid aspirated from different experimental groups). B) Percentage of cell death (values were means of five replicates). Data were expressed as mean \pm SE. *** significant compared to EAC at $P < 0.001$.

by TLC with visualization by UV irradiation.

3.2. General procedure for synthesis of compound Ia and IIa

To 4.76 g BtH (40 mmol) dissolved in 50 cm³ CH₂Cl₂, 0.73 cm³ SOCl₂ (10 mmol) were added. The mixture was stirred at 25 °C for 30 min, followed by the addition of the corresponding acid (10 mmol) and the reaction was allowed to stir for an additional 3 hrs at 25 °C. The reaction was diluted with 50 cm³ CH₂Cl₂ and the organic layer was washed with saturated Na₂CO₃ (3 \times 20 cm³), 20 cm³ H₂O, and 10 cm³ brine. The organic layer was dried over anhydrous sodium sulfate, 50 cm³ hexane was added to the filtrate, and then the solid obtained was dried under vacuum to give compound Ia and IIa.

3.3. General procedure for Synthesis of target compounds II and IIIa-g

The corresponding amino acids (5 mmol) was dissolved in water (3 mL) with 1 equivalent triethylamine (5 mmol, 70 mL) and added to the solution of the *N*-acylbenzotriazoles Ia or IIa (5 mmol) in CH₃CN (9 mL) or Dioxane (9 mL). The mixture was stirred for 5hrs at room temperature but in case of anthranilic acid heating at 60 °C was needed (until complete consumption of *N*-acylbenzotriazole as monitored by TLC). The pH was adjusted to 5 using 2 N HCl, and the solvent was evaporated under reduced pressure. The residue was then extracted with ethyl acetate (2 \times 20 mL) and the organic layer was washed with 4 N HCl (3 \times 10 mL), water (10 mL), and brine (10 mL) then dried over anhydrous sodium sulfate. The organic layer was evaporated under reduced pressure to give the desired compounds II and IIIa-g.

3.3.1. (1H-Benzo[d][1,2,3]triazol-1-yl)(4-chlorophenyl)methanone (Ia)

White microcrystals, yield 2.4 g (93 %); mp 138–140 °C (138–139 °C) [49].

3.3.2. (4-Chlorobenzoyl)-L-methionine II

White microcrystals, yield 1.28 g (89%); mp 101–103 °C. ¹H NMR

(400 MHz, DMSO-*d*₆) δ 8.77 (d, $J = 7.6$ Hz, 1H, NH), 7.93 (d, $J = 8.4$ Hz, 2H, OC-*ortho*-Ar-H), 7.57 (d, $J = 8.4$ Hz, 2H, CO-*meta*-Ar-H), 4.54 (q, $J = 8.0$ Hz, 1H, -NH-CH-), 2.65–2.56 (m, 2H, -CH₂-SCH₃), 2.10–2.06 (m, 5H, -CH₂-CH₂-SCH₃). ¹³C NMR (100 MHz, DMSO-*d*₆) δ 174.0 (COOH), 167.2 (CO), 134.4 (=C-Cl), 131.9 (=C-CO), 128.7 (Ar-C), 127.9 (Ar-C), 52.1 (-CH-COOH), 30.7 (-CH₂CH₂SCH₃), 30.6 (-CH₂CH₂SCH₃), 15.1 (-SCH₃). HRMS (ESI): m/z calcd for C₁₂ H₁₅ Cl N O₃ S ([M+H]⁺) 288.0456, found 288.0462.

3.3.3. (S)-N-(1-(1H-benzo[d][1,2,3]triazol-1-yl)-4-(methylthio)-1-oxobutan-2-yl)-4-chlorobenzamide (IIa)

White microcrystals, yield 3.46 g (89%); mp 78–80 °C. ¹H NMR (400 MHz, DMSO-*d*₆) δ 9.34 (d, $J = 6.4$ Hz, 1H, NH), 8.31 (d, $J = 8.0$ Hz, 1H, Ar-H), 8.25 (d, $J = 8.0$ Hz, 1H, Ar-H), 7.97 (d, $J = 8.4$ Hz, 2H, OC-*ortho*-Ar-H), 7.82 (t, $J = 7.6$ Hz, 1H, Ar-H), 7.66 (t, $J = 7.6$ Hz, 1H, Ar-H), 7.60 (d, $J = 8.4$ Hz, 2H, OC-*meta*-Ar-H), 5.99–5.94 (m, 1H, -CH-), 2.82 (dd, $J = 7.6, 5.2$ Hz, 1H, -CH₂SCH₃), 2.73 (dd, $J = 13.2, 7.6$ Hz, 1H, -CH₂SCH₃), 2.41–2.30 (m, 2H, -CH₂CH₂SCH₃), 2.10 (s, 3H, -SCH₃). ¹³C NMR (100 MHz, DMSO-*d*₆) δ 171.9 (-CO-N-), 166.8 (-CONH), 145.8 (-N=N-C), 137.2 (=C-Cl), 132.3 (=C-CO), 131.6 (Ar-C), 131.2 (Ar-C), 130.1 (Ar-C), 129.0 (Ar-C), 127.2 (Ar-C), 120.7 (Ar-C), 114.5 (Ar-C), 53.3 (-CH-), 30.4 (-CH₂CH₂SCH₃), 29.8 (CH₂CH₂SCH₃), 14.8 (-SCH₃). Anal. Calcd. for C₁₈H₁₇ClN₄O₂S: C, 55.60; H, 4.41; N, 14.41, S, 8.24 found C, 55.70; H, 4.47; N, 14.43, S, 8.28

3.3.4. (4-Chlorobenzoyl)-L-methionylglycine IIIa

White microcrystals, yield 1.57 g (91%); mp 161–163 °C. ¹H NMR (400 MHz, DMSO-*d*₆) δ 12.64 (s, 1H, COOH), 8.68 (d, $J = 8.0$ Hz, 1H, NHCH₂), 8.35 (s, 1H, NHCH-), 7.95 (d, $J = 8.4$ Hz, 2H, Ar-H), 7.56 (d, $J = 8.4$ Hz, 2H, Ar-H), 4.58 (dd, $J = 13.4, 8.2$ Hz, 1H, CH), 3.82 (dd, $J = 17.6, 5.8$ Hz, 1H, NHCH₂), 3.73 (dd, $J = 17.6, 5.6$ Hz, 1H, NHCH₂), 2.61–2.54 (m, 2H, -CH₂SCH₃), 2.06 (s, 3H, SCH₃), 2.02–1.95 (m, 2H, -CHCH₂-). ¹³C NMR (100 MHz, DMSO-*d*₆) δ 172.2 (COOH), 171.6 (CHCO), 165.9 (=C-CO), 136.6 (Cl-C=), 133.2 (COC=), 130.1 (Ar-C), 128.7 (Ar-C), 53.1 (CH), 41.2 (NHCH₂), 31.8 (CHCH₂), 30.4 (SCH₂), 15.1 (SCH₃). HRMS (ESI): m/z calcd for C₁₄ H₁₈ Cl N₂ O₄ S ([M+H]⁺) 345.067, found 345.06809.

3.3.5. (4-Chlorobenzoyl)-L-methionyl-L-methionine (IIIb)

Oily, yield 1.72 g (82%). ¹H NMR (400 MHz, DMSO-*d*₆) δ 12.64 (s, 1H, COOH), 8.78 (d, $J = 7.6$ Hz, 1H, -NH-CO-C=), 8.38 (d, $J = 8.4$ Hz, 1H, -NH-CH-COOH), 7.93 (d, $J = 8.0$ Hz, 2H, -CO-*ortho*-Ar-H), 7.57 (d, $J = 8.0$ Hz, 2H, -CO-*meta*-Ar-H), 4.56–4.49 (m, 1H, -CH-), 4.37–4.32 (m, 1H, -CH-), 3.10–3.05 (m, 1H, CH₂SCH₃), 2.63–2.54 (m, 3H, CH₂SCH₃), 2.07–2.02 (m, 10H, 2(-CH₂CH₂SCH₃)). ¹³C NMR (100 MHz, DMSO-*d*₆) δ 173.9 (COOH), 172.0 (-NH-CO-CH-), 166.1 (-CO-C=), 136.7 (Cl-C=), 133.1 (-CO-C=), 129.9 (Ar-C), 128.8 (Ar-C), 52.2 (-CH-), 45.9 (CH-), 31.0 (Aliph-C), 30.5 (Aliph-C), 30.3 (Aliph-C), 30.1 (Aliph-C), 15.0 (-SCH₃), 9.0 (-SCH₃). HRMS (ESI): m/z calcd for C₁₇ H₂₄ Cl N₂ O₄ S₂ ([M+H]⁺) 419.0861, found 419.08717.

3.3.6. (4-Chlorobenzoyl)-L-methionyl-L-cysteine (IIIc)

Oily, yield 1.56 g (80%). ¹H NMR (400 MHz, DMSO-*d*₆) δ 8.78 (d, $J = 8$ Hz, 1H, -NH-CO-C=), 7.97 (s, 1H, NH), 7.93 (d, $J = 8.8$ Hz, 2H, -CO-*ortho*-Ar-H), 7.57 (d, $J = 8.8$ Hz, 2H, -CO-*meta*-Ar-H), 4.65–4.50 (m, 2H, -CH-), 3.31 (dd, $J = 14.4, 5.2$ Hz, 1H, HS-CH₂-), 3.08 (dd, $J = 7.2, 5.2$ Hz, 1H, HS-CH₂-), 2.65–2.54 (m, 2H, -CH₂-SCH₃), 2.10–2.07 (m, 5H, -CH₂CH₂SCH₃), 1.20 (s, 1H, SH). ¹³C NMR (100 MHz, DMSO-*d*₆) δ 173.9 (COOH), 166.9 (NHCOCH-), 166.1 (=C-CO), 136.7 (Cl-C=), 133.1 (Ar-C), 129.7 (Ar-C), 128.8 (Ar-C), 52.2 (CH-COOH), 45.9 (NH-CH-CONH-), 30.6 (Aliph-C), 30.5 (Aliph-C), 28.9 (Aliph-C), 15.0 (-SCH₃). Anal. Calcd. for C₁₅H₁₉ClN₂O₄S₂: C, 46.09; H, 4.90; N, 7.17; S, 16.40 found C, 46.18; H, 4.97; N, 7.17; S, 16.49

3.3.7. (4-Chlorobenzoyl)-L-methionyl-L-histidine (**III d**)

Oily, yield 1.76 g (83%). ^1H NMR (400 MHz, DMSO- d_6) δ 10.51 (s, 1H, NH), 9.05 (s, 1H, $-\text{CH}=\text{N}-$), 8.78 (d, $J = 7.6$ Hz, 1H, $-\text{NH}-\text{CO}-\text{C}=\text{C}-$), 8.66 (d, $J = 7.2$ Hz, 1H, $-\text{NH}-\text{CH}-\text{COOH}$), 7.96 (d, $J = 8.4$ Hz, 2H, $-\text{CO}-\text{ortho}(\text{Ar}-\text{H})$), 7.55 (d, $J = 8.4$ Hz, 2H, $-\text{CO}-\text{meta}(\text{Ar}-\text{H})$), 7.46 (s, 1H, $-\text{NH}-\text{CH}=\text{N}-$), 4.59–4.47 (m, 2H, $-\text{CH}-$), 3.21 (dd, $J = 15.6, 5.2$ Hz, 1H, $-\text{CH}_2-\text{CH}-\text{COOH}$), 3.04 (d, br, 1H, $-\text{CH}_2-\text{CH}-\text{COOH}$), 2.56–2.42 (m, 2H, $-\text{CH}_2\text{SCH}_3$), 2.04–1.92 (m, 5H, $-\text{CH}_2\text{CH}_2\text{SCH}_3$). ^{13}C NMR (100 MHz, DMSO- d_6) δ 172.4 (COOH), 172.0 ($-\text{NH}-\text{CO}-\text{CH}-$), 166.0 ($-\text{CO}-\text{C}=\text{C}-$), 136.7 (Cl- $\text{C}=\text{C}-$), 133.8 ($-\text{C}=\text{N}-$), 133.1 (Ar-C), 130.13 (Ar-C), 130.1 (Ar-C), 128.7 (Ar-C), 117.4 (Ar-C), 53.4 ($-\text{CHCOOH}$), 45.8 ($-\text{NHCHCO}-$), 31.6 (Aliph-C), 30.3 (Aliph-C), 15.1 (Aliph-C), 8.9 ($-\text{SCH}_3$). HRMS (ESI): m/z calcd for $\text{C}_{18}\text{H}_{22}\text{Cl N}_4\text{O}_4\text{S}$ ($[\text{M}+\text{H}]^+$) 425.1045, found 425.11029.

3.3.8. (4-Chlorobenzoyl)-L-methionyl-L-phenylalanine (**III e**)

Oily, yield 1.85 g (85%). ^1H NMR (400 MHz, DMSO- d_6) δ 12.83 (s, 1H, COOH), 8.77 (d, $J = 7.6$ Hz, 1H, $=\text{C}-\text{CO}-\text{NH}-$), 8.33 (d, $J = 8.0$ Hz, 1H, NHCHCOOH), 7.93 (d, $J = 8.4$ Hz, 2H, $-\text{CO}-\text{ortho}(\text{Ar}-\text{H})$), 7.57 (d, $J = 8.4$ Hz, 2H, $-\text{CO}-\text{meta}(\text{Ar}-\text{H})$), 7.34–7.21 (m, 5H, Ar-H), 4.56–4.43 (m, 2H, 2CH), 3.11–3.05 (m, 1H, $=\text{C}-\text{CH}_2-$), 2.98–2.89 (m, 1H, $=\text{C}-\text{CH}_2-$), 2.65–2.56 (m, 2H, SCH_2-), 2.07 (s, 3H, SCH_3), 2.01–1.83 (m, 2H, SCH_2CH_2). ^{13}C NMR (100 MHz, DMSO- d_6) δ 173.9 (COOH), 173.3 (CHCONH), 166.1 ($=\text{C}-\text{CO}$), 137.9 (Cl- $\text{C}=\text{C}$), 136.7 (Ar-C), 133.1 (Ar-C), 129.9 (Ar-C), 129.6 (Ar-C), 128.8 (Ar-C), 128.7 (Ar-C), 126.9 (Ar-C), 52.2 (CH-COOH), 46.0 ($-\text{NH}-\text{CO}-\text{CH}-$), 31.9 ($=\text{C}-\text{CH}_2$), 30.6 (SCH_2CH_2), 27.2 (SCH_2-), 15.0 (SCH_3). HRMS (ESI): m/z calcd for $\text{C}_{21}\text{H}_{24}\text{Cl N}_2\text{O}_4\text{S}$ ($[\text{M}+\text{H}]^+$) 435.114, found 435.11496.

3.3.9. (4-Chlorobenzoyl)-L-methionyl-L-arginine (**III f**)

Oily, yield 1.93 g (87%). ^1H NMR (400 MHz, DMSO- d_6) δ 8.83 (d, $J = 7.2$ Hz, 1H, $=\text{C}-\text{CO}-\text{NH}-$), 8.48 (d, $J = 7.2$ Hz, 1H, $-\text{NH}-\text{CH}-\text{COOH}$), 7.95 (d, $J = 7.6$ Hz, 2H, $-\text{CO}-\text{ortho}-\text{Ar}-\text{H}$), 7.56–7.09 (m, 5H, $-\text{CO}-\text{meta}-\text{Ar}-\text{H}$, NH_2 , $=\text{NH}$), 4.62–4.51 (m, 1H, $-\text{CH}-\text{COOH}$), 4.18 (s, br, 1H, $=\text{C}-\text{CO}-\text{NH}-\text{CH}-$), 3.75–3.62 (m, 2H, $-\text{NH}-\text{CH}_2-$), 3.12 (s, br, 2H, CH_2SCH_3), 2.06 (s, br, 5H, $-\text{CH}_2\text{CH}_2\text{SCH}_3$), 1.72 (d, br, 2H, CH_2CHCOOH), 1.53 (d, br, 2H, $-\text{CH}_2\text{CH}_2\text{CHCOOH}$), 1.22 (s, 1H, NH). ^{13}C NMR (100 MHz, DMSO- d_6) δ 173.8 (COOH), 172.0 ($-\text{NHCOC}-$), 166.1 ($=\text{C}-\text{CO}-$), 157.6 (C=NH), 136.7 (Cl- $\text{C}=\text{C}$), 133.2 ($-\text{CO}-\text{C}=\text{C}$), 130.1 (Ar-C), 128.7 (Ar-C), 53.5 ($=\text{C}-\text{CONHCH}-$), 52.2 ($-\text{CHCOOH}$), 40.7 ($-\text{CH}_2\text{NHC}=\text{NH}$), 32.1 (Aliph-C), 30.6 (Aliph-C), 28.5 (Aliph-C), 25.7 (Aliph-C), 15.2 (SCH_3). HRMS (ESI): m/z calcd for $\text{C}_{18}\text{H}_{27}\text{Cl N}_5\text{O}_4\text{S}$ ($[\text{M}+\text{H}]^+$) 444.1467, found 444.14801.

3.3.10. (S)-2-(2-(4-Chlorobenzamido)-4-(methylthio)butanamido)benzoic acid **III g**

Buff microcrystals, yield 1.67 g (82%); mp 205–207 °C. ^1H NMR (400 MHz, DMSO- d_6) δ 11.80 (s, 1H, COOH), 9.15 (s, 1H, $=\text{C}-\text{NH}$), 8.67 (d, $J = 8.4$ Hz, 1H, $-\text{CH}-\text{NH}-$), 8.03–7.98 (m, 3H, Ar-H), 7.64–7.54 (m, 3H, Ar-H), 7.17 (t, $J = 7.4$ Hz, 1H, $-\text{NH}-\text{para}-\text{Ar}-\text{H}$), 4.71–4.65 (m, 1H, $-\text{NH}-\text{CH}-$), 2.67–2.57 (m, 2H, $-\text{CH}_2-\text{SCH}_3-$), 2.31–2.12 (m, 2H, $-\text{CH}_2\text{CH}_2\text{SCH}_3$), 2.08 (s, 3H, $-\text{SCH}_3$). ^{13}C NMR (100 MHz, DMSO- d_6) δ 171.3 ($-\text{CO}-\text{NH}-\text{C}=\text{C}-$), 170.0 ($-\text{COOH}$), 166.7 ($-\text{NH}-\text{CO}-\text{C}=\text{C}-$), 141.1 ($-\text{NH}-\text{C}=\text{C}-$), 136.9 (Cl- $\text{C}=\text{C}$), 134.8 (Ar-C), 132.9 (Ar-C), 131.7 (Ar-C), 130.2 (Ar-C), 128.8 (Ar-C), 123.3 (Ar-C), 119.9 (Ar-C), 116.5 (Ar-C), 54.7 ($-\text{CH}-\text{CO}-$), 30.7 ($-\text{CH}_2\text{CH}_2\text{SCH}_3$), 30.6 ($-\text{CH}_2\text{CH}_2\text{SCH}_3$), 15.00 ($-\text{SCH}_3$). HRMS (ESI): m/z calcd for $\text{C}_{19}\text{H}_{20}\text{Cl N}_2\text{O}_4\text{S}$ ($[\text{M}+\text{H}]^+$) 407.0827, found 407.08352.

3.4. Oxidative stress biomarkers evaluation

LLC-PK1 cells were pretreated 1/3 IC_{50} of the most potent targets **II**, **III b** and **III g** respectively for 8 h, followed by addition of 4 μM of CP and the mixture was left for 24 h to evaluate Oxidative stress biomarkers namely, GSH/GSSG ratio, ROS, SOD and MDA) as follow

3.5. Measurement of GSH/GSSG ratio

The GSH/GSSG ratio was determined following a method previously described by Irfan Rahman and his coworkers [50].

3.6. Measurement of ROS production

Human reactive oxygen species (ROS) ELISA Kit (BIOASSAY TECHNOLOGY – CHINA) that uses a double-antibody sandwich enzyme-linked immunosorbent assay (ELISA) to assay the level of reactive oxygen species (ROS) was used following manufacturer's instructions.

3.7. Measurement of SOD and MDA

The SOD and MDA activity were determined according to the instructions of the assay kits (Lifespan Biosciences, Seattle, USA).

4. Conclusions

We have designed and synthesized a novel nephroprotective peptidomimetic having the ability to attenuate CP-induced nephrotoxicity probably by acting as guardians against oxidative stress. Among the synthesized compounds, **III g** showed the most potent renoprotective effect with antioxidant activity supported by invivo improvement in results of renal function tests and attenuated CP-induced renal structural injury in Sprague Dawley rats, proper physicochemical and pharmacokinetic properties. Moreover, **III g** did not affect CP chemotherapeutic effect both *in vivo* and *in vitro*. Thus, *N-p-chlorobenzoyl-Methionyl anthranilic acid* (**III g**), *N-p-chlorobenzoyl-Met-OH* (**II**) and *N-p-chlorobenzoyl-Met-Met-OH* (**III b**) are promising candidate compounds for further investigation to develop better renoprotective agents.

Declaration of Competing Interest

The authors declare that they have no known competing financial interests or personal relationships that could have appeared to influence the work reported in this paper.

Acknowledgements

We thank HRMS facility, Faculty of pharmacy, Fayoum University, Egypt, for mass analysis.

Appendix A. Supplementary material

Full experimental detail, ^1H and ^{13}C NMR spectra can be found via the “Supplementary Content” section of this article's webpage. Supplementary data to this article can be found online at <https://doi.org/10.1016/j.bioorg.2021.105100>.

References

- [1] S. Dasari, P.B. Tchounwou, Cisplatin in Cancer Therapy: Molecular Mechanisms of Action, Eur. J. Pharmacol. 740 (2014) 364–378, <https://doi.org/10.1016/j.ejphar.2014.07.025>.
- [2] R. Galgamuwa, K. Hardy, J.E. Dahlstrom, A.C. Blackburn, E. Wium, M. Rooke, J. Y. Cappello, P. Tummala, H.R. Patel, A. Chuah, L. Tian, L. McMorro, P.G. Board, A. Theodoratos, Dichloroacetate Prevents Cisplatin-Induced Nephrotoxicity without Compromising Cisplatin Anticancer Properties, J. Am. Soc. Nephrol. 27 (11) (2016) 3331–3344, <https://doi.org/10.1681/ASN.2015070827>.
- [3] M. Perše, Ž. Večerić-Haler, Cisplatin-Induced Rodent Model of Kidney Injury: Characteristics and Challenges, Biomed Res. Int. 2018 (2018) 1462802, <https://doi.org/10.1155/2018/1462802>.
- [4] R.P. Miller, R.K. Tadagavadi, G. Ramesh, W.B. Reeves, Mechanisms of Cisplatin Nephrotoxicity, Toxins (Basel). 2 (11) (2010) 2490–2518, <https://doi.org/10.3390/toxins2112490>.
- [5] M.H. Hanigan, P. Devarajan, Cisplatin Nephrotoxicity: Molecular Mechanisms, Cancer Ther. 1 (2003) 47–61. PMID:PMC2180401.
- [6] Y.I. Chirino, J. Pedraza-Chaverri, Role of Oxidative and Nitrosative Stress in Cisplatin-Induced Nephrotoxicity, Exp. Toxicol. Pathol. Off. J. Gesellschaft fur

- Toxicologische Pathol. 61 (3) (2009) 223–242, <https://doi.org/10.1016/j.etp.2008.09.003>.
- [7] J. Kulbacka, J. Saczko, A. Chwilkowska, Oxidative stress in cells damage processes, *Pol. Merk. Lekarski* 27 (157) (2009) 44–47. PMID:19650429.
- [8] S. Hajian, M. Rafieian-Kopaei, H. Nasri, Renoprotective Effects of Antioxidants against Cisplatin Nephrotoxicity, *J. Nephropharmacol.* 3 (2) (2014) 39–42. PMID: 28197460.
- [9] A. Stefanucci, R. Costante, G. Macedonio, S. Dvoracsko, A. Mollica, Cysteine-, Methionine- and Seleno-Cysteine-Proline Chimeras: Synthesis and Their Use in Peptidomimetics Design, *Curr. Bioact. Compd.* 3 (12) (2016) 200–206, <https://doi.org/10.2174/1573407212666160511162915>.
- [10] A. Stefanucci, M.P. Dimmito, G. Tenore, S. Pieretti, P. Minosi, G. Zengin, C. Sturaro, G. Calò, E. Novellino, A. Cichelli, A. Mollica, Plant-derived peptides rubiscolin-6, soymorphin-6 and their c-terminal amide derivatives: Pharmacokinetic properties and biological activity, *J. Funct. Foods* 73 (2020) 104154, <https://doi.org/10.1016/j.jff.2020.104154>.
- [11] J. Tokunaga, M. Kobayashi, A. Kitagawa, C. Nakamura, K. Arimori, M. Nakano, Protective Effects of N-Benzoyl Amino Acids on Cisplatin Nephrotoxicity in Rats, *Biol. Pharm. Bull.* 19 (11) (1996) 1451–1456, <https://doi.org/10.1248/bpb.19.1451>.
- [12] R. Kröning, A.K. Lichtenstein, G.T. Nagami, Sulfur-Containing Amino Acids Decrease Cisplatin Cytotoxicity and Uptake in Renal Tubule Epithelial Cell Lines, *Cancer Chemother. Pharmacol.* 45 (1) (2000) 43–49, <https://doi.org/10.1007/PL00006741>.
- [13] C. Schoneich, F. Zhao, G.S. Wilson, R.T. Borchardt, Iron-Thiolate Induced Oxidation of Methionine to Methionine Sulfoxide in Small Model Peptides. Intramolecular Catalysis by Histidine, *Biochim. Biophys. Acta* 1158 (3) (1993) 307–322, [https://doi.org/10.1016/0304-4165\(93\)90030-c](https://doi.org/10.1016/0304-4165(93)90030-c).
- [14] N. Brot, H. Weissbach, Biochemistry and Physiological Role of Methionine Sulfoxide Residues in Proteins, *Arch. Biochem. Biophys.* 223 (1) (1983) 271–281, [https://doi.org/10.1016/0003-9861\(83\)90592-1](https://doi.org/10.1016/0003-9861(83)90592-1).
- [15] R.L. Levine, B.S. Berlett, J. Moskowitz, L. Moseni, E.R. Stadtman, Methionine Residues May Protect Proteins from Critical Oxidative Damage, *Mech. Ageing Dev.* 107 (3) (1999) 323–332, [https://doi.org/10.1016/s0047-6374\(98\)00152-3](https://doi.org/10.1016/s0047-6374(98)00152-3).
- [16] V.K. Singh, K. Singh, K. Baum, The Role of Methionine Sulfoxide Reductases in Oxidative Stress Tolerance and Virulence of *Staphylococcus Aureus* and Other Bacteria, *Antioxidants (Basel, Switzerland)* 7 (10) (2018), <https://doi.org/10.3390/antiox7100128>.
- [17] F. Cabreiro, C.R. Picot, B. Friguet, I. Petropoulos, Methionine Sulfoxide Reductases: Relevance to Aging and Protection against Oxidative Stress, *Ann. N. Y. Acad. Sci.* 1067 (2006) 37–44, <https://doi.org/10.1196/annals.1354.006>.
- [18] P.M. Deegan, L.S. Pratt, M.P. Ryan, The Nephrotoxicity, Cytotoxicity and Renal Handling of a Cisplatin-Methionine Complex in Male Wistar Rats, *Toxicology* 89 (1) (1994) 1–14, [https://doi.org/10.1016/0300-483x\(94\)90128-7](https://doi.org/10.1016/0300-483x(94)90128-7).
- [19] M. Sooriyaarachchi, W.M. White, A. Narendran, J. Gailer, Chemoprotection by D-Methionine against Cisplatin-Induced Side-Effects: Insight from in Vitro Studies Using Human Plasma, *Metallomics* 6 (3) (2014) 532–541, <https://doi.org/10.1039/c3mt00238a>.
- [20] M.A.K. Azad, S. Sivanesan, J. Wang, K. Chen, R.L. Nation, P.E. Thompson, K. D. Roberts, T. Velko, J. Li, Methionine Ameliorates Polymyxin-Induced Nephrotoxicity by Attenuating Cellular Oxidative Stress, *Antimicrob. Agents Chemother.* 62 (1) (2018), <https://doi.org/10.1128/AAC.01254-17>.
- [21] M. Nematbakhsh, Z. Pezeshki, F. Eshraghi Jazi, B. Mazaheri, M. Moeni, T. Safari, F. Azarkish, F. Moslemi, M. Maleki, A. Rezaei, S. Saberi, A. Dehghani, M. Malek, A. Mansouri, M. Ghasemi, F. Zeinali, Z. Zamani, M. Navidi, S. Jilanchi, S. Shirdavani, F. Ashrafi, Cisplatin-Induced Nephrotoxicity; Protective Supplements and Gender Differences, *Asian Pac. J. Cancer Prev.* 18 (2) (2017) 295–314. <https://doi.org/10.22034/APJCP.2017.18.2.295>.
- [22] J.M. Dennis, P.K. Witting, Protective Role for Antioxidants in Acute Kidney Disease, *Nutrients* 9 (7) (2017) 718, <https://doi.org/10.3390/nu9070718>.
- [23] M.K. Unnikrishnan, M.N.A. Rao, Antiinflammatory Activity of Methionine, Methionine Sulfoxide and Methionine Sulfone, *Agents Actions* 31 (1) (1990) 110–112, <https://doi.org/10.1007/BF02003229>.
- [24] A.R. Katritzky, K. Suzuki, Z. Wang, Acylbenzotriazoles as Advantageous N-, C-, S-, and O-Acylating Agents, *Synlett* 2005 (11) (2005) 1656–1665, <https://doi.org/10.1055/s-2005-871551>.
- [25] N.E. Abo-Dya, S. Biswas, A. Basak, I. Avan, K.A. Alamry, A.R. Katritzky, Benzotriazole-Mediated Synthesis of Aza-Peptides: En Route to an Aza-Leu-enkephalin Analogue, *J. Org. Chem.* 78 (8) (2013) 3541–3552, <https://doi.org/10.1021/jo302251e>.
- [26] G. Klopman, L.R. Stefan, R.D. Saiakhov, ADME Evaluation. 2. A Computer Model for the Prediction of Intestinal Absorption in Humans, *Eur. J. Pharm. Sci.* 17 (4–5) (2002) 253–263, [https://doi.org/10.1016/s0928-0987\(02\)00219-1](https://doi.org/10.1016/s0928-0987(02)00219-1).
- [27] J.H. Lin, A.Y. Lu, Role of Pharmacokinetics and Metabolism in Drug Discovery and Development, *Pharmacol. Rev.* 49 (4) (1997) 403–449. PMID:9443165.
- [28] F. Lombardo, P.V. Desai, R. Arimoto, K.E. Desino, H. Fischer, C.E. Keefer, C. Petersson, S. Winiwarter, F. Broccatelli, In Silico Absorption, Distribution, Metabolism, Excretion, and Pharmacokinetics (ADME-PK): Utility and Best Practices. An Industry Perspective from the International Consortium for Innovation through Quality in Pharmaceutical Development, *J. Med. Chem.* 60 (22) (2017) 9097–9113, <https://doi.org/10.1021/acs.jmedchem.7b00487>.
- [29] C.A. Lipinski, F. Lombardo, B.W. Dominy, P.J. Feeney, Experimental and Computational Approaches to Estimate Solubility and Permeability in Drug Discovery and Development Settings, *Adv. Drug Deliv. Rev.* 46 (1–3) (2001) 3–26, [https://doi.org/10.1016/s0169-409x\(00\)00129-0](https://doi.org/10.1016/s0169-409x(00)00129-0).
- [30] A. Daina, O. Michielin, V. Zoete, SwissADME: A Free Web Tool to Evaluate Pharmacokinetics, Drug-Likeness and Medicinal Chemistry Friendliness of Small Molecules, *Sci. Rep.* 7 (2017), <https://doi.org/10.1038/srep42717>.
- [31] J. Pizzorno, *Glutathione*, *Integr. Med. (Encinitas)* 13 (1) (2014) 8–12. PMID: 26770075.
- [32] J.B. Owen, D.A. Butterfield, Measurement of Oxidized/Reduced Glutathione Ratio 2020, 269–277. https://doi.org/10.1007/978-1-60761-756-3_18.
- [33] I. Németh, D. Boda, The Ratio of Oxidized/reduced Glutathione as an Index of Oxidative Stress in Various Experimental Models of Shock Syndrome, *Biomed. Biochim. Acta* 48 (2–3) (1989) S53–7. PMID:2730630.
- [34] H. Younus, Therapeutic Potentials of Superoxide Dismutase, *Int. J. Health Sci. (Qassim)* 12 (3) (2018) 88–93. PMID:29896077.
- [35] C.A. Davis, H.S. Nick, A. Agarwal, Manganese Superoxide Dismutase Attenuates Cisplatin-Induced Renal Injury: Importance of Superoxide, *J. Am. Soc. Nephrol.* 12 (12) (2001) 2683. LP-2690. PMID:11729237.
- [36] F. Kuyumcu, A. Aycan, Evaluation of Oxidative Stress Levels and Antioxidant Enzyme Activities in Burst Fractures, *Med. Sci. Monit. Int. Med. J. Exp. Clin. Res.* 24 (2018) 225–234. <https://doi.org/10.12659/msm.908312>.
- [37] M.K. Jafari, K. Ansarin, A. Jouyban, Comments on “Use of Malondialdehyde as a Biomarker for Assessing Oxidative Stress in Different Disease Pathologies” A Review, *Iran. J. Public Health* 44 (2015) 714–715. PMID:26284218.
- [38] A.R. Alhoshani, M.M. Hafez, S. Husain, A.M. Al-shaikh, M.R. Alotaibi, S.S. Al Rejaie, M.A. Alshammari, M.M. Almutairi, O.A. Al-Shabanah, Protective Effect of Rutin Supplementation against Cisplatin-Induced Nephrotoxicity in Rats, *BMC Nephrol.* 18 (1) (2017) 194, <https://doi.org/10.1186/s12882-017-0601-y>.
- [39] M. Schieber, N.S. Chandel, ROS Function in Redox Signaling and Oxidative Stress, *Curr. Biol.* 24 (10) (2014) R453–R462, <https://doi.org/10.1016/j.cub.2014.03.034>.
- [40] S.J. Holditch, C.N. Brown, A.M. Lombardi, K.N. Nguyen, C.L. Edelstein, Recent Advances in Models, Mechanisms, Biomarkers, and Interventions in Cisplatin-Induced Acute Kidney Injury, *Int. J. Mol. Sci.* 20 (12) (2019) 3011, <https://doi.org/10.3390/ijms20123011>.
- [41] N.M. Elsherbiny, M. Al-Gayyar, M Anti-tumor activity of arjunolic acid against Ehrlich Ascites Carcinoma cells in vivo and in vitro through blocking TGF- β type 1 receptor, *Biomed Pharmacother.* 82 (2016) 28–34, <https://doi.org/10.1016/j.biopha.2016.04.046>.
- [42] N.N. Younis, N.M. Elsherbiny, M.A. Shaheen, M.M. Elseweidy, Modulation of NADPH Oxidase and Nrf2/HO-1 Pathway by Vanillin in Cisplatin-Induced Nephrotoxicity in Rats, *J. Pharm. Pharmacol.* 72 (11) (2020) 1546–1555, <https://doi.org/10.1111/jphp.13340>.
- [43] N. Ma, W. Wei, X. Fan, X. Ci, Farrerol Attenuates Cisplatin-Induced Nephrotoxicity by Inhibiting the Reactive Oxygen Species-Mediated Oxidation, Inflammation, and Apoptotic Signaling Pathways, *Front. Physiol.* 10 (2019) 1419, <https://doi.org/10.3389/fphys.2019.01419>.
- [44] L.M. Aleksunes, M.J. Goedken, C.E. Rockwell, J. Thomale, J.E. Manautou, C. D. Klaassen, Transcriptional Regulation of Renal Cytoprotective Genes by Nrf2 and Its Potential Use as a Therapeutic Target to Mitigate Cisplatin-Induced Nephrotoxicity, *J. Pharmacol. Exp. Ther.* 335 (1) (2010) 2–12, <https://doi.org/10.1124/jpet.110.170084>.
- [45] Z. Wang, W. Sun, X. Sun, Y. Wang, M. Zhou, Kaempferol Ameliorates Cisplatin Induced Nephrotoxicity by Modulating Oxidative Stress, Inflammation and Apoptosis via ERK and NF- κ B Pathways, *AMB Express* 10 (1) (2020) 58, <https://doi.org/10.1186/s13568-020-00993-w>.
- [46] Z. Wang, M. Liang, H. Li, L. Cai, H. He, Q. Wu, L. Yang, L-Methionine Activates Nrf2-ARE Pathway to Induce Endogenous Antioxidant Activity for Depressing ROS-Derived Oxidative Stress in Growing Rats, *J. Sci. Food Agric.* 99 (10) (2019) 4849–4862, <https://doi.org/10.1002/jsfa.9757>.
- [47] N.H. Eisa, N.M. Elsherbiny, A.M. Shebl, L.A. Eissa, M.M. El-Shishtawy, Phenethyl isothiocyanate potentiates anti-tumour effect of doxorubicin through Akt-dependent pathway, *Cell Biochem. Funct.* 33 (8) (2015) 541–551, <https://doi.org/10.1002/cbf.3153>.
- [48] M.A. Mansour, W.M. Ibrahim, E.S. Shalaan, A.F. Salama, Combination of arsenic trioxide and cisplatin synergistically inhibits both hexokinase activity and viability of Ehrlich ascites carcinoma cells, *J. Biochem. Mol. Toxicol.* 33 (8) (2019), e22350, <https://doi.org/10.1002/jbt.22350>.
- [49] A.R. Katritzky, A.V. Vakulenko, R. Jain, The Preparation of N-Acylbenzotriazoles from Aldehydes, *Arkivoc* 2003 (xiv) (2003) 131–139, <https://doi.org/10.3998/ark.5550190.0004.e12>.
- [50] I. Rahman, A. Kode, S.K. Biswas, Assay for Quantitative Determination of Glutathione and Glutathione Disulfide Levels Using Enzymatic Recycling Method, *Nat. Protoc.* 1 (6) (2006) 3159–3165, <https://doi.org/10.1038/nprot.2006.378>.